RED CELLS, IRON, AND ERYTHROPOIESIS

Activation of the erythroid K-Cl cotransporter Kcc1 enhances sickle cell disease pathology in a humanized mouse model

Fiona C. Brown,[1] Ashlee J. Conway,[1] Loretta Cerruti,[1] Janelle E. Collinge,[2] Catriona McLean,[3] James S. Wiley,[4] Ben T. Kile,[2] Stephen M. Jane,[1,3,5,*] and David J. Curtis[1,3,*]

[1]Australian Centre for Blood Diseases, Central Clinical School, Monash University, Melbourne, Australia; [2]Cancer and Haematology Division, The Walter and Eliza Hall Institute of Medical Research, Parkville, Australia; [3]The Alfred Hospital, Melbourne, Australia; [4]The Florey Institute of Neuroscience and Mental Health, University of Melbourne, Parkville, Australia; and [5]Department of Medicine, Central Clinical School, Monash University, Melbourne, Australia

Key Points

- A missense mutation in the cytoplasmic tail of Kcc1 activates K-Cl cotransporter activity by impairing phosphorylation of nearby threonines.
- In vivo evidence shows that activation of Kcc1 directly contributes to the pathogenesis of sickle cell disease.

We used an N-ethyl-N-nitrosurea-based forward genetic screen in mice to identify new genes and alleles that regulate erythropoiesis. Here, we describe a mouse line expressing an activated form of the K-Cl cotransporter Slc12a4 (Kcc1), which results in a semi-dominant microcytosis of red cells. A missense mutation from methionine to lysine in the cytoplasmic tail of Kcc1 impairs phosphorylation of adjacent threonines required for inhibiting cotransporter activity. We bred *Kcc1*^{M935K} mutant mice with a humanized mouse model of sickle cell disease to directly explore the relevance of the reported increase in KCC activity in disease pathogenesis. We show that a single mutant allele of *Kcc1* induces widespread sickling and tissue damage, leading to premature death. This mouse model reveals important new insights into the regulation of K-Cl cotransporters and provides in vivo evidence that increased KCC activity worsened end-organ damage and diminished survival in sickle cell disease. (*Blood*. 2015;126(26):2863-2870)

Introduction

The maintenance of intracellular Cl^- concentration is critical for the normal function of many physiologic processes, including regulation of red cell volume.[1] Intracellular Cl^- concentration is controlled in part by the K-Cl cotransporters, which pump Cl^- and K^+ ions with the obligatory movement of water out of the cell. The K-Cl cotransporters are encoded by 4 different genes of the SLC12A electroneutral cation-chloride family: KCC1 (SLC12A4), KCC2 (SLC12A5), KCC3 (SLC12A6), and KCC4 (SLC12A7). KCC1 and KCC3 are the predominant K-Cl cotransporters in red cells, with KCC1 expression highest in reticulocytes, and KCC3 expression relatively constant throughout erythroid maturation.[2] Gene targeting studies in the mouse show that red cell K-Cl cotransport is mediated predominantly by KCC3.[3]

The major mechanism regulating the activity of the K-Cl cotransporters is a coordinated cascade of phosphorylation and dephosphorylation events, which have been defined by studying the rate of K-Cl cotransport in response to inhibitors of protein (serine/threonine and tyrosine) kinases and protein phosphatases.[4-7] A number of studies have demonstrated that the stimulation of K-Cl cotransport during hypotonicity is mediated via protein phosphatases (such as PP1, PP2A, and PP2B), because the protein phosphatase inhibitor calyculin A is able to ablate K-Cl cotransport activation. In contrast, the broad-range protein kinase inhibitor staurosporine and the kinase inhibitor *N*-ethylmaleimide are potent stimulators of K-Cl cotransport. Under basal (isotonic) conditions, the KCCs are highly phosphorylated, and thus, K-Cl cotransport is minimal. The targets of phosphorylation include 2 threonine residues within the C-terminal cytoplasmic domain of KCC3, T991, and T1048, which share sequence conservation across all KCCs.[8] Silent interfering RNA for the no-lysine kinase member WNK1 partially blocked phosphorylation at these sites,[8] consistent with previous reports that the WNK family mediate KCC phosphorylation.[5,9] Recently, the WNK-regulated SPAK/OSR1 kinases were demonstrated to directly phosphorylate and inhibit KCC3 activity at specific threonine residues including T1048 but not T991.[10] A better understanding of how KCC activity is regulated will provide new therapeutic avenues for modulating epithelial and neuronal ion transport in human diseases such as hypertension and epilepsy.

Sickle cell disease (SCD), resulting from an inherited point mutation in the sixth codon of the human β-globin genes, is characterized by a chronic hemolytic anemia with episodes of painful vaso-occlusive crises induced by dehydration and infection. Red cell dehydration is a key precipitant of sickle hemoglobin (HbS) polymerization, leading to the formation of irreversible, sickle-shaped red cells with microvascular occlusion and chronic organ damage. One potential

Submitted October 30, 2014; accepted September 24, 2015. Prepublished online as *Blood* First Edition paper, October 8, 2015; DOI 10.1182/blood-2014-10-609362.

*S.M.J. and D.J.C. contributed equally to this work.

The online version of this article contains a data supplement.

There is an Inside *Blood* Commentary on this article in this issue.

The publication costs of this article were defrayed in part by page charge payment. Therefore, and solely to indicate this fact, this article is hereby marked "advertisement" in accordance with 18 USC section 1734.

contributor to red cell dehydration in sickle red cells is increased activity of KCCs.[11,12] Therapeutic inhibition of KCC activity is a proposed strategy to increase red cell hydration and reduce the frequency of sickle crises, although specific and potent small molecule inhibitors of KCCs have not yet been developed. To address the therapeutic potential of inhibiting KCCs, investigators have used a humanized mouse model of SCD (SAD mice), which has increased erythroid KCC activity but has a relatively mild phenotype.[13] Gene deletion of *Kcc1* and *Kcc3* improved red cell hydration of sickle red cells, but did not significantly improve the anemia or the proportion of the most dehydrated red cells.[3] Effects on end-organ damage were not evaluated, in part because Kcc3$^{-/-}$ mice have severe neurodegeneration.[14] Therefore, it remains unclear whether activation of KCC directly contributes to crises in SCD.

To identify dominant mutations affecting erythropoiesis, we undertook a large-scale dominant N-ethyl-N-nitrosurea (ENU) mutagenesis screen in mice.[15,16] In this study, we report a mouse line expressing an activating mutant allele of *Kcc1* (*Kcc1*^{M935K}), which leads to microcytic red cells. This nonconservative amino acid substitution leads to Kcc1 activation by impairing phosphorylation of the C-terminal cytoplasmic threonines homologous to those identified in KCC3. We use this mouse line to provide in vivo evidence that increased activity of Kcc1 contributes to end-organ damage and diminished survival in SCD.

Materials and methods

Mice

A G1 pedigree (RBC10; KCC1^{M935K}) displaying microcytosis was identified in a dominant ENU mutagenesis screen on a C57BL/6J background as described previously.[15,16] KCC1^{M935K} mice were maintained on a mixed C57BL/6J × BALB/c background because the microcytic phenotype was less severe when backcrossed onto a pure C57BL/6J background. Mice were genotyped by polymerase chain reaction (PCR) amplification of the region spanning the M935K mutation using primers: forward (5′-AGCTGAAGTG GAGGTGGTAGAGAT-3′) and reverse (5′-TCCAGCCTAAGAGCCGAG TG-3′), followed by sequencing the PCR product using the Big Dye Terminator reagents (Australian Genome Research Facility) to identify the point mutation. The humanized sickle strain developed by Dr Tim Townes [B6;129-Hbatm1(HBA)Tow Hbbtm2(HBG1,HBB*)Tow/Hbbtm3(HBG1, HBB)Tow/J; strain 013071] was obtained from The Jackson Laboratory as Ha/Ha::$\beta^A\beta^S$ animals. These animals lack all mouse globins and are homozygous for the human hemoglobin α gene and contain 1 allele of the human hemoglobin β gene and 1 allele of the human hemoglobin β-sickle gene. The strain was maintained through heterozygous intercrossing of Ha/Ha::$\beta^A\beta^S$ animals. The Sickle/KCC1 strain was produced by mating Sickle heterozygous mice (Ha/Ha::$\beta^A\beta^S$) with KCC1$^{M935K/M935K}$ mice to produce F1 progeny heterozygous for the humanized globin alleles and heterozygous for the KCC1 allele. Breeding of the F1 progeny yielded animals homozygous for the humanized globin genes and lacking all mouse globins. The Kcc1/Sickle strain was maintained by mating Ha/Ha::$\beta^A\beta^S$ _KCC1$^{+/M935K}$ animals. Genotyping sickle animals was performed using a 3-PCR method outlined on the Jackson Laboratories Web site for this strain. Littermate controls were used for all analyses. The Animal Ethics Committees of the University of Melbourne and the Alfred Medical Research and Education Precinct approved all animal experiments.

Gene mapping, genomic custom-capture array, and next-generation sequencing

Mapping was performed by outcrossing affected heterozygotes to wild-type Balb/c mice. Tail genomic DNA from G2 and subsequent generation animals was subjected to simple sequence length polymorphism-based genome-wide scanning and single nucleotide polymorphism (SNP) fine mapping. A genomic custom capture array was constructed by Roche-NimbleGen to preferentially enrich the candidate interval from 105.92 to 109.15 Mb on chromosome 8. Massively parallel sequencing was performed using the Illumina HiSeq platform with the C57BL/6 reference sequence used for assembly and alignment of the reads obtained from sequencing, which identified a point mutation at position 2804 of Slc12a4 (Kcc1: NC_000074.6), resulting in a methionine to lysine substitution at amino acid 935.

HEK293 cells expressing Kcc1 or Kcc3

The Flp-In T-rex 293 system (Invitrogen) was used for the expression of N-terminally HA-tagged mouse Kcc1 or Kcc3b according to the manufacturer's instructions. Mouse *Kcc1* and *Kcc3* cDNA were cloned into the tetracycline-inducible pcDNA5/FRT/TO-TOPO TA vector (Invitrogen) by PCR amplification and pTOPO (Invitrogen) cloning for use in the expression system. Mutations were introduced by oligonucleotide-based site-directed mutagenesis. Cells were maintained in Dulbecco's modified Eagle medium containing 10% fetal bovine serum, 100 μg/mL hygromycin, and 5 μg/mL blasticidin. Three days before the addition of tetracycline for gene expression, the media were changed to tetracycline-free media (Dulbecco's modified Eagle medium containing no fetal bovine serum) to limit basal expression of mKCC1 and mKCC3b in the absence of tetracycline. Gene expression was induced by the addition of 1 μg/mL tetracycline for 24 hours, which was verified by quantitative PCR and western blotting against HA.

^{86}Rb flux assays

Blood was collected from experimental animals by cardiac puncture into lithium heparin vaccutainer blood collection tubes (BD Biosciences) and washed in 150 mM NaCl. Red cells were placed in isotonic flux buffer (140 mM NaCl, 5.5 mM KCl, 20 mM 2-[4-(2-hydroxyethyl)piperazin-1-yl]ethanesulfonic acid free acid, 5.5 mM D-glucose, and 0.1% bovine serum albumin; pH 7.45) and loaded with 20 μCi ^{86}Rb at 37°C for at least 2 hours. Cells were washed twice in ice cold 150 mM NaCl, followed by a final wash in the buffer to be used in K^+ efflux. For K^+ efflux, cells were resuspended at 37°C in either isotonic or hypotonic flux buffer (100 mM NaCl, 5.5 mM KCl, 20 mM 2-[4-(2-hydroxyethyl)piperazin-1-yl]ethanesulfonic acid free acid, 5.5 mM D-glucose, and 0.1% bovine serum albumin, pH 7.45). All reactions contained 0.1 mM oubain octahydrate (to inhibit the ATPase/K pump) and 10 μM bumetanide (to inhibit NKCC1 and NKCC2). Aliquots of cells were removed at 20, 40, and 60 minutes and centrifuged, and the supernatant was harvested for analysis on a Wallac Wizard Automatic γ Counter. At the completion of efflux, an aliquot of cells was reserved for the measurement of intracellular ^{86}Rb. The percentage of K^+ in supernatants was normalized to the intracellular ^{86}Rb count, and K^+ efflux was represented as the percentage of change compared with the 0-minute time point. Additional inhibitors included 50 μM calyculin A to inhibit protein phosphatases responsible for the hypotonic stimulation of K-Cl cotransporter activity.

Potassium cotransport in HEK293 cells overexpressing HA-mKcc1 and HA-mKcc3 mutants was measured using ^{86}Rb influx experiments. Cells were grown on poly-L-lysine (Sigma)–coated 12-well cell culture plates. After gene expression was induced, cells were preincubated in 1 mL isotonic or hypotonic flux buffer containing 0.1 mM oubain octahydrate and 10 μM bumetanide at 37°C for 10 minutes. Influx was initiated by the addition of 5 μCi ^{86}Rb, which occurred over 2 and 10 minutes. After this time, cells were and allowed to dry on a nitrocellulose Hybond-C membrane, which was exposed to Amersham Hyperfilm ECL (GE Healthcare) for up to 24 hours at −80°C. The remaining cells were diluted in 10 μL 0.4% trypan blue solution (Gibco) for cell counting. Potassium influx was assessed by measuring the level of ^{86}Rb autoradiography measured by densitometry using Adobe Photoshop Elements relative to cell number.

Results

Characterization of a mouse line with microcytic anemia

Using ENU mutagenesis to discover new alleles that regulate erythropoiesis,[15] we identified a mouse (*RBC10*) in the first generation

Table 1. Full blood examination of RBC10 mice

	+/+	RBC10$^{+/m}$	RBC10$^{m/m}$
Hemoglobin (g/dL)	16.66 ± 0.51	15.87 ± 0.39*	15.33 ± 0.55*
Red cells (×10^{12}/L)	11.17 ± 0.32	12.31 ± 0.47*	13.61 ± 0.40*†
Hematocrit (%)	49.71 ± 0.95	48.23 ± 1.59*	47.51 ± 1.96*†
MCV (fl)	44.52 ± 0.84	39.20 ± 0.67*	34.91 ± 0.92*†
MCH (pg)	14.90 ± 0.56	12.91 ± 0.37*	11.26 ± 0.33*†
MCHC (g/dL)	33.45 ± 0.81	32.95 ± 0.80	32.31 ± 1.01
RDW (%)	15.97 ± 1.81	18.05 ± 1.20*	19.45 ± 0.89*†
Reticulocytes (%)	2.68 ± 0.53	2.74 ± 0.60	3.0 ± 0.50
Platelets (×10^{9}/L)	1007 ± 98	1020 ± 116	1113 ± 119
White cells (×10^{9}/L)	8.48 ± 1.38	8.23 ± 2.27	10.36 ± 3.02
Ferritin (μg/L)	1815 ± 191	ND	1560 ± 175

Blood parameters obtained from 7-week-old male wild-type (+/+, n = 12), RBC10 heterozygous (n = 19), and RBC10 homozygous (n = 11) mice. Means ± SDs are shown. MCHC, mean corpuscular hemoglobin concentration; ND, not done; RDW, red cell distribution width.

*$P < .05$ compared with WT mice, two-tailed Student *t* test.

†$P < 0.05$ compared with RBC10$^{+/m}$ mice, two-tailed Student *t* test.

(G1) with a mean cell volume (MCV) >3 standard deviations (SDs) below the normal (MCV, 39 vs 45 fl in wild-type mice). Fifty percent of pups born from affected mice crossed with wild-type mice displayed a reduced MCV, indicating that the phenotype was fully penetrant (data not shown). Approximately one quarter of mice born from intercrosses of *RBC10* heterozygotes (*RBC10*$^{+/m}$) had a more severe red cell phenotype, suggesting that homozygotes (*RBC10*$^{m/m}$) were viable (Table 1). *RBC10*$^{m/m}$ mice had mild anemia with a markedly reduced MCV and mean cell hemoglobin (MCH), indicative of a microcytic, hypochromic anemia (Table 1). Leukocyte and platelet counts were normal. Peripheral blood smears revealed microcytic red cells with occasional target cells (Figure 1A). Iron deficiency and thalassemia, the most common causes of microcytic hypochromic anemia, were unlikely because *RBC10*$^{m/m}$ mice had normal serum ferritin (Table 1), and there was no evidence of α:β globin chain imbalance (supplemental Figure 1A available on the *Blood* Web site). Osmotic fragility analysis of *RBC10* mutant red cells displayed reduced lysis in a gene dose-dependent manner (Figure 1B). Furthermore, the density distribution of *RBC10* mutant red cells was shifted toward higher densities, indicating impaired steady-state volume homeostasis (Figure 1C). Surprisingly, this was observed in the setting of unchanged MCHCs in the mutant cells. Finally, there was no evidence of hemolysis: reticulocyte count was normal (Table 1), splenic erythropoiesis was normal in quantity and differentiation supplemental Figure 1B-C), and in vivo survival of *RBC10*$^{m/m}$ red cells was normal (supplemental Figure 1D). Overall, these analyses demonstrate a microcytic hypochromic anemia with increased red cell density.

RBC10 is a point mutation in the potassium chloride cotransporter, Kcc1

The gene mutation was mapped by crossing *RBC10*$^{+/m}$ mice on a C57BL/6 genetic background with wild-type BALB/c mice. Genome-wide and fine mapping of SNPs based on low MCV localized the mutation to a region lying between 108.31 and 109.15 Mb on chromosome 8 (Figure 2A). Massively parallel sequencing of a 3.65-Mb custom-capture genomic array spanning this region identified a T to A substitution at nucleotide position 2804 in exon 21 of *Kcc1*. Sanger sequencing of presumed heterozygous and homozygous RBC10 mice based on phenotype showed exact correlation between severity and the number of mutant *Kcc1* alleles (Figure 2B). The point mutation was predicted to generate a missense mutation from methionine to lysine at amino acid 935 (M935K). Quantitative real-time PCR analysis demonstrated comparable levels of *Kcc1* mRNA in wild-type and homozygous mice, indicating that the mutation had no effect on RNA stability (Figure 2C). Expression of Kcc3, the other major Kcc in

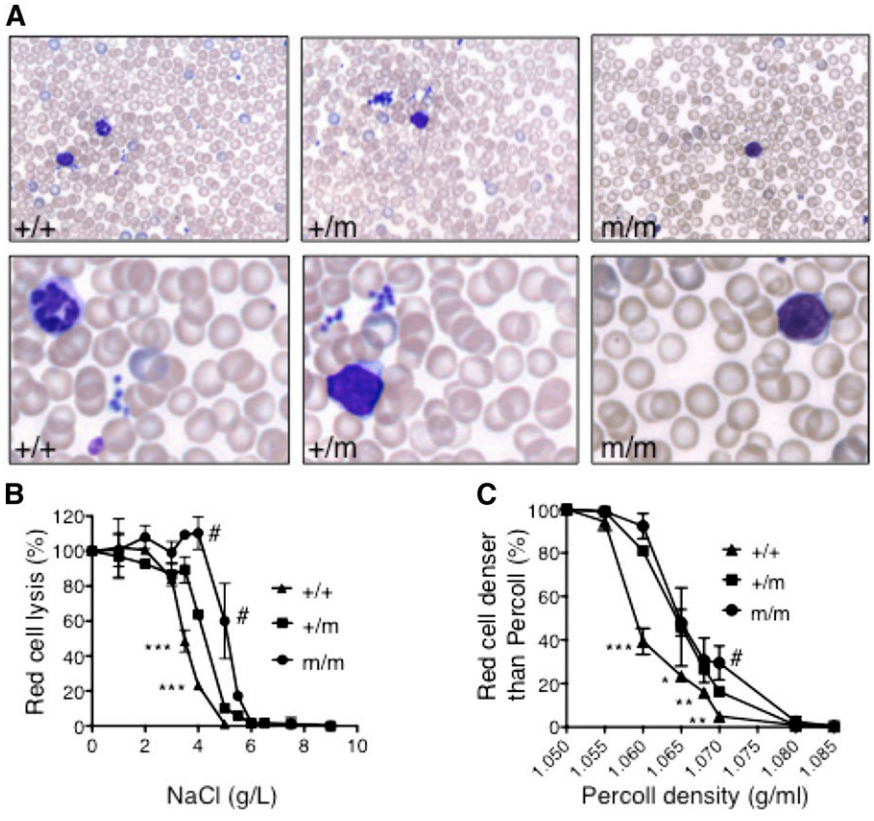

Figure 1. Red cell characteristics of RBC10 mice. (A) Peripheral blood smears from 7-week-old wild-type (+/+), RBC10 heterozygous (+/m), and homozygous (m/m) mice. (B) Osmotic fragility shows significantly reduced sensitivity of RBC10 mutant red cells. Plots are representative of 2 independent experiments using 3 animals of each genotype. (C) Red cell densities of wild-type, RBC10 heterozygous, and RBC homozygous mice determined by centrifugation through Percoll mixture of defined density. Student *t* test: wild type compared with RBC10 heterozygous: *$P < .05$, **$P < .01$, ***$P < .001$. RBC10 homozygous compared with heterozygous: #$P < .05$.

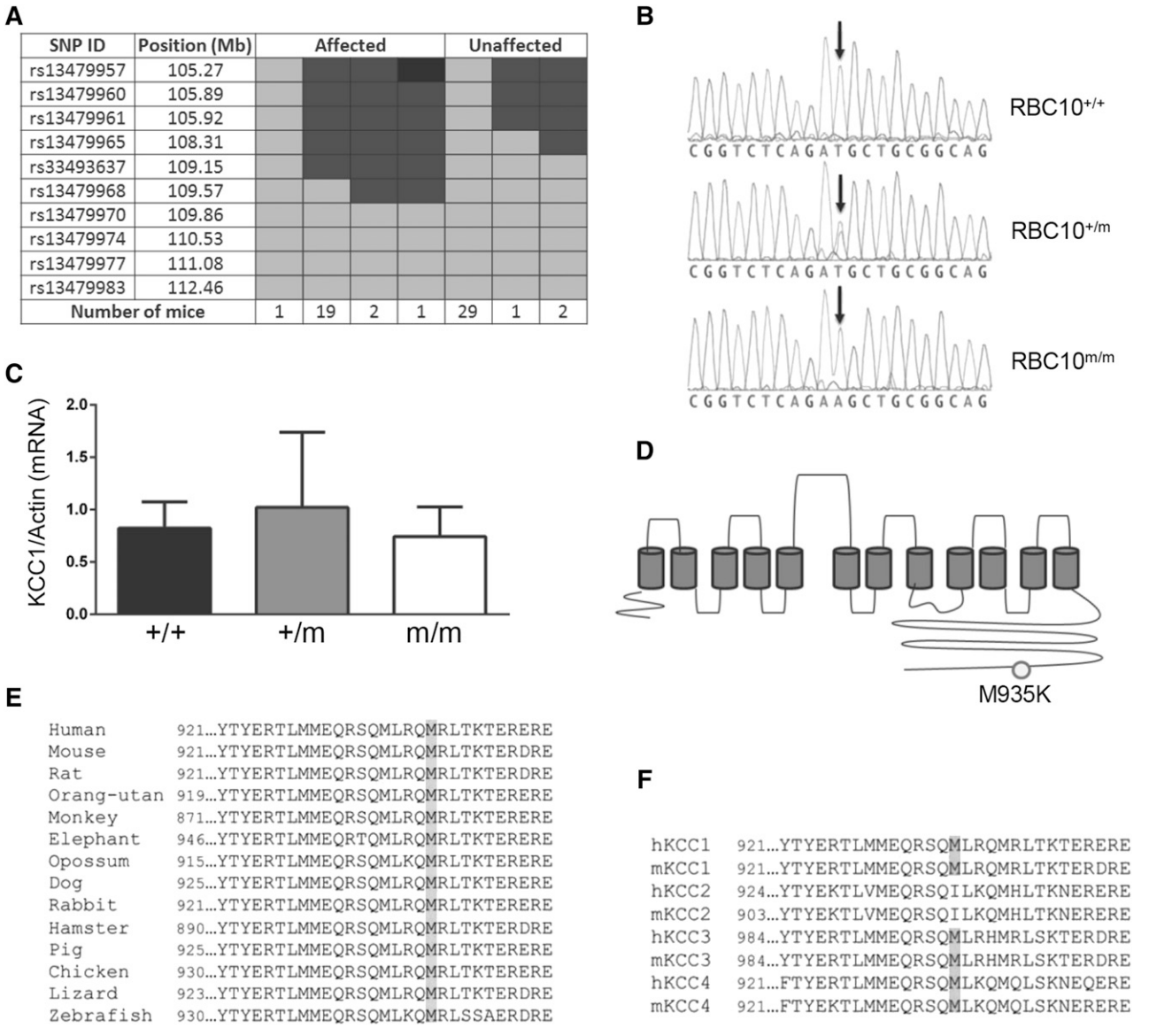

Figure 2. Identification of a missense mutation in the cytoplasmic domain of *Kcc1*. (A) Fine SNP mapping of 55 mice at 10 SNP markers localized in the RBC10 mutation between 105.92 and 109.15 Mb on chromosome 8. Light gray, homozygous for BALB/c; dark gray, heterozygous for BALB/c and C57BL/6; black, homozygous for C57BL/6. (B) DNA sequence results showing the T to A base substitution of *Kcc1*. (C) Quantitative reverse transcriptase-PCR for *Kcc1* mRNA expression in the spleen. Mean ± SD for 3 age-matched mice of each genotype. (D) Schematic of Kcc1 protein showing the M935K mutation. (E) The M935 residue and adjacent amino acids display significant homology across vertebrate evolution, and (F) the human and mouse KCC family members.

erythrocytes, was also unaffected by the Kcc1 mutation (supplemental Figure 2). The M935K mutation resides in the C-terminal cytoplasmic domain of Kcc1 (Figure 2D), within a region highly conserved across vertebrate evolution (Figure 2E), and the 4 mammalian KCC proteins (Figure 2F).

M935K mutation leads to activation of KCC1 activity

To investigate the effect of the M935K mutation on K-Cl cotransport, we measured ^{86}Rb efflux by heterozygous and homozygous mutant ($Kcc1^{M935/M935K}$) red cells. Under isotonic conditions, which do not stimulate K-Cl cotransport, the $Kcc1^{M935K/M935K}$ red cells displayed a twofold increase in ^{86}Rb efflux compared with normal red cells, suggesting the M935K mutation causes activation of K-Cl cotransport. $Kcc1^{+/M935K}$ heterozygous red cells had an intermediate activated phenotype (Figure 3A).

To explore the mechanism of this activation, we tested the response of red cells to hypotonicity, which normally induces activation of KCC1 by dephosphorylation.[8] As expected, ^{86}Rb efflux by wild-type red cells was stimulated by hypotonicity, and this response was blocked by treatment with the phosphatase inhibitor calyculin A (Figure 3B). In contrast, hypotonic conditions had no stimulatory effect on ^{86}Rb efflux by $Kcc1^{M935K/M935K}$ red cells, suggesting that the mutant Kcc1 already existed in a dephosphorylated state. The activated state of $Kcc1^{M935K/M935K}$ red cells could be restored to normal basal levels by calyculin A, indicating that in the absence of phosphatase activity, the Kcc1^{M935K} mutation did not preclude phosphorylation of KCC1.

To demonstrate that the M935K mutation intrinsically activated Kcc1, we generated stable HEK293 cell lines expressing tetracycline-inducible HA-tagged Kcc1 wild type (HA-Kcc1 WT) or M935K (HA-Kcc1 M935K). Western blot analysis demonstrated similar expression levels of wild-type and mutant Kcc1 in the presence of

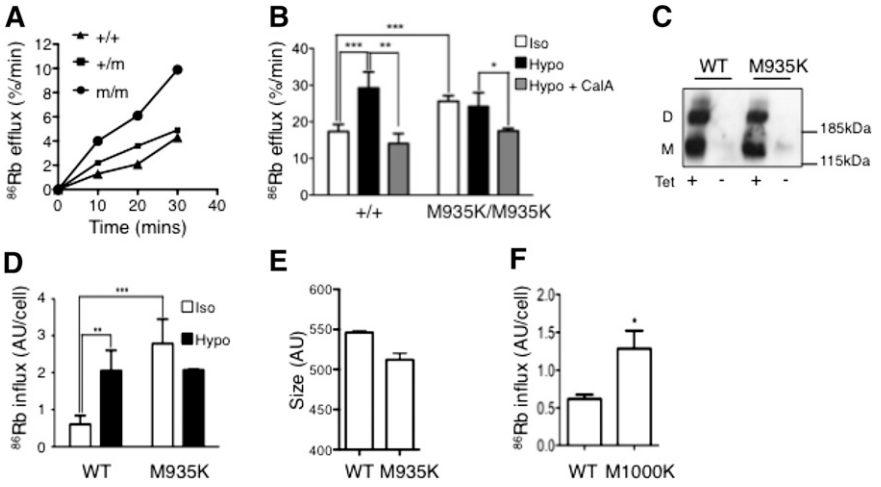

Figure 3. The M935K mutation increases KCC1 cotransporter activity. (A) ^{86}Rb efflux over time for red blood cells in isotonic conditions in the presence of oubain and bumetanide. (B) ^{86}Rb efflux assays demonstrating increased efflux from $Kcc1^{M935K/M935K}$ red cells in isotonic (iso) but not hypotonic (hypo) conditions and is reversible by the phosphatase inhibitor, calyculin A (CalA). Mean ± SD representative of 2 independent experiments from 3 mice of each genotype. (C) Western blot (anti-HA) from HEK293 cells transfected with tetracycline-inducible vector expressing wild-type (WT) or M935K mutant hemagglutinin (HA)-tagged Kcc1. (D) ^{86}Rb influx over 2 minutes in HEK293 cells expressing WT or M935K Kcc1. Results are the mean ± SD of 3 independent experiments of cells grown in duplicate relative to the non–tetracycline-induced cells. (E) Size of HEK293 cells expressing WT or M935K Kcc1 measured by forward scatter. Results are the mean ± SD of 3 independent experiments of cells grown in tetracycline. (F) ^{86}Rb influx over 2 minutes in HEK293 cells expressing WT or M1000K HA-tagged Kcc3 in isotonic conditions. Results are the mean ± SD of 2 independent experiments of cells grown in duplicate. Student *t* test: $^{*}P < .05$; $^{**}P < .01$; $^{***}P < .001$.

tetracycline (Figure 3C). Immunofluorescence confirmed cell membrane expression of the M935K mutant similar to wild-type Kcc1 (supplemental Figure 3). To measure the effect of Kcc1 mutation on K-Cl cotransporter activity, we used ^{86}Rb influx, as the efflux assay used for red cells was insensitive in HEK293 cells (data not shown). Consistent with our findings in red cells, HA-Kcc1 M935K-expressing cells displayed a four- to fivefold increase in ^{86}Rb influx compared with HA-Kcc1 WT-expressing cells (Figure 3D). In addition, the M935K mutant was insensitive to stimulation by hypotonic stress (Figure 3D). Moreover, HEK293 cells expressing Kcc1 M935K displayed reduced cell size analogous to the small red cells seen in $Kcc1^{M935K/M935K}$ mice (Figure 3E). Finally, HEK293 cells transfected with KCC3 mutated at the homologous methionine residue also demonstrated activation of K-Cl cotransporter activity (Figure 3F). These results confirm that the M935K mutation in KCC1 is responsible for constitutive activation of KCC1.

M935K mutation impairs phosphorylation of neighboring regulatory threonines

KCC3 activity is tightly regulated by phosphorylation of 2 conserved threonines: T991 and T1048.[8] Therefore, we postulated that the M935K mutation might activate KCC1 by perturbing phosphorylation of these nearby threonine residues (Figure 4A). We first confirmed that the homologous threonine residues were important for activity of KCC1 using the HEK293 inducible system. Similar to the M935K mutation, KCC1 containing the single threonine mutants, T926A and T983A, showed constitutive activation of KCC1 activity in isotonic conditions (ninefold and fivefold increase, respectively), which did not further increase with hypotonicity (Figure 4B). Consistent with the synergistic effects reported for KCC3,[8] the KCC1 double threonine mutants (T926A/T983A) displayed markedly elevated KCC1 activity (16-fold increase) compared with the wild-type control cells. A similar synergistic effect was observed with KCC1 double mutants containing the M935K mutation (T926A/M935K and M935K/T983A). Thus, activation of K-Cl cotransport by the M935K mutation in KCC1 was mediated through a threonine phosphorylation-dependent mechanism.

Phospho-antibodies to T991 and T1048 of KCC3 did not recognize the homologous threonines of murine Kcc1. Therefore, to directly determine the impact of the M935K mutation on threonine phosphorylation of Kcc1, we used the HA-tagged Kcc1-expressing HEK293 cell lines. Western blotting of immunoprecipitates with anti-phospho-threonine antibody demonstrated a modest but reproducible reduction in threonine phosphorylation in M935K-expressing cells (57% of wild-type levels; Figure 4C). This decrease was observed in both the monomeric and dimeric forms of Kcc1. Western blotting of immunoprecipitates with anti-HA confirmed similar pull down of HA-tagged KCCs. Reduced threonine phosphorylation was observed in both T926A and T983A mutants, with T926A most strongly reduced. This was consistent with the findings of Rinehart and coworkers,[8] which found T991 of KCC3 (the homologous threonine to T926 of KCC1) to be the major target of phosphorylation. Consistent with the synergistic effects on KCC activity of the M935K mutation with either of the threonine mutants, threonine phosphorylation was dramatically reduced in all double mutants (19-26% of wild-type levels) and almost completely inhibited in the triple mutant (5% of wild-type levels). Finally, threonine phosphorylation was similarly reduced in the M1000K mutant of KCC3 (Figure 4D), demonstrating that the homologous site in KCC3 is also a critical residue for K-Cl cotransport regulation. In summary, these findings support a model in which the M935K mutation imparts constitutive activation of KCC1 by impairing phosphorylation of key regulatory threonines (Figure 4E).

Activated KCC1 directly aggravates SCD

Dehydration of red cells is a major determinant of HbS polymerization in SCD, leading to complications including pulmonary hypertension, stroke, and leg ulcers. KCC activity is increased in sickle red cells, which may contribute to red cell dehydration and sickling, although the impact of increased KCC activity on the clinical severity of SCD has not been directly addressed. Therefore, we used the knockin mouse model of SCD (Hb^{SS}), which phenocopies many of the features of human disease including severe anemia and crises.[17] $Hb^{AS}KCC1^{+/M935K}$ mice were generated by crossing $KCC1^{+/M935K}$ mice with Hb^{AS} mice for

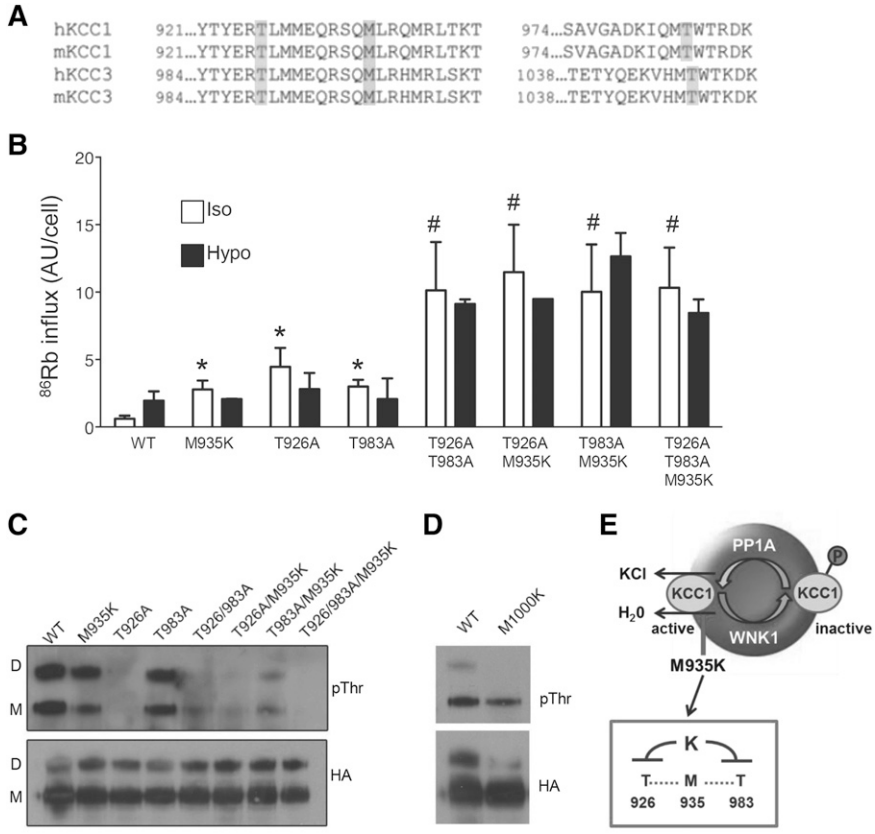

Figure 4. M935K mutation impairs phosphorylation of threonines in the cytoplasmic tail of Kcc1. (A) Alignment of human and mouse KCC1 and KCC3 showing sites of conserved methionine in relation to known regulatory threonines. (B) ^{86}Rb influx in HEK293 cells expressing wild-type Kcc1 (WT) or various Kcc1 mutants in isotonic and hypotonic conditions. $^{*}P < .05$ compared with WT; $^{\#}P < .05$ compared with M935K. (C) Western blot of anti-HA immunoprecipitates probed with anti-phosphothreonine (pThr) or anti-HA antibodies. D, dimer; M, monomer. (D) Western blot of anti-HA immunoprecipitates from HEK293 cells expressing wild-type or the homologous Kcc3 mutant M1000K demonstrating impaired phospho-threonine. (E) A schematic illustrating the regulation of KCC1 and the inhibitory effect of M935K mutation on nearby threonines leading to constitutive activation of K-Cl cotransport.

2 generations to eliminate all mouse globin alleles carried by the KCC1^{M935K} line. Mating of sickle/Kcc1^{M935K} heterozygous mice (*Hb^{AS}Kcc1$^{+/M935K}$*) with sickle heterozygous/Kcc1^{M935K} homozygous mice (*Hb^{AS}KCC1$^{M935K/M935K}$*) demonstrated reduced numbers of *Hb^{SS}Kcc1$^{M935K/M935K}$* mice at 10 days of age (Table 2). Analysis of blood counts in adult mice surviving to 10 weeks of age revealed increased anemia in sickle heterozygous mice homozygous for mutant Kcc1 (*Hb^{AS}KCC1$^{M935K/M935K}$*) and sickle homozygous mice heterozygous for mutant Kcc1 (*Hb^{SS}KCC1$^{+/M935K}$*; Figure 5A; supplemental Table 1). Only a single homozygous sickle homozygous mutant Kcc1 (*Hb^{SS}KCC1$^{M935K/M935K}$*) survived to 10 weeks of age. The presence of a single Kcc1 mutant allele increased reticulocytes and spleen size ($9.4 \pm 0.3\%$ of body weight compared with $4.6 \pm 0.5\%$ in *Hb^{SS}Kcc1$^{+/+}$* mice) in sickle homozygous mice but had no significant effect in sickle heterozygous mice (Figure 5B-C). In the setting of sickle homozygosity, the presence of a single mutant Kcc1 allele markedly shortened survival (median 134 days for *Hb^{SS}KCC1$^{+/M935K}$* mice) compared with sickle homozygous mice expressing wild-type Kcc1 (median 258 days; Figure 5D).

We used the ^{86}Rb efflux assays to assess the effect of mutant Kcc1 on KCC activity in sickle red cells. As previously reported, sickle red cells had increased KCC activity (^{86}Rb efflux in $Hb^{SS} > Hb^{AS} > Hb^{AA}$; Figure 5E). The presence of a single Kcc1 mutant allele increased KCC activity in sickle homozygous red cells, although this may be explained by the increased reticulocytes in these mice (Figure 5B). In the setting of sickle heterozygous red cells where reticulocytes were not increased, homozygous Kcc1 mutation significantly increased KCC activity (Figure 5E). Heterozygous Kcc1 mutation increased the red cell density of sickle heterozygous red cells, thereby linking increased Kcc1 activity to increased red cell density of sickle red cells.

Finally, we examined histologic sections of organs from 10-week-old mice to understand the effect of increased KCC activity on end-organ damage (Figure 6). The most profound difference was seen in the lungs where *Hb^{SS}Kcc1$^{+/M935K}$* mice exhibited more marked interstitial congestion and more intra-alveolar leakage of red cells. In the kidney, *Hb^{SS}Kcc1$^{+/M935K}$* mice displayed mesangial proliferation and more red cells in the tubules. Finally, in the liver, centrilobular necrosis and congestion, more marked lobular inflammation, and numerous sickle cells in the sinusoids were evident. Taken together, our results show that activation of KCC1 directly aggravates SCD.

Discussion

Here, we describe a unique mouse line with a point mutation of the K-Cl cotransporter *Kcc1*. We show that a missense mutation from methionine to lysine in the cytoplasmic tail of Kcc1 leads to increased cotransporter activity and consequently microcytic red cells with increased density. Studies using an inducible expression vector in HEK cells show that this mutation impairs phosphorylation of regulatory threonines required for inhibiting K-Cl cotransport. We used this mouse line to demonstrate that increased K-Cl cotransporter

Table 2. Genotypes of 10-day-old offspring

	Sickle genotype					
	AA	AA	AS	AS	SS	SS
Kcc1 genotype	+/M	M/M	+/M	M/M	+/M	M/M
Expected %	12.5	12.5	25	25	12.5	12.5
Observed n (%)	13 (19%)	13 (19%)	13 (19%)	17 (25%)	10 (15%)	3 (4%)*

Offspring generated by mating Hb^{AS} Kcc1$^{+/M935K}$ mice with Hb^{AS} Kcc1$^{M935K/M935K}$ mice.

*χ^2 test: $P = .001$.

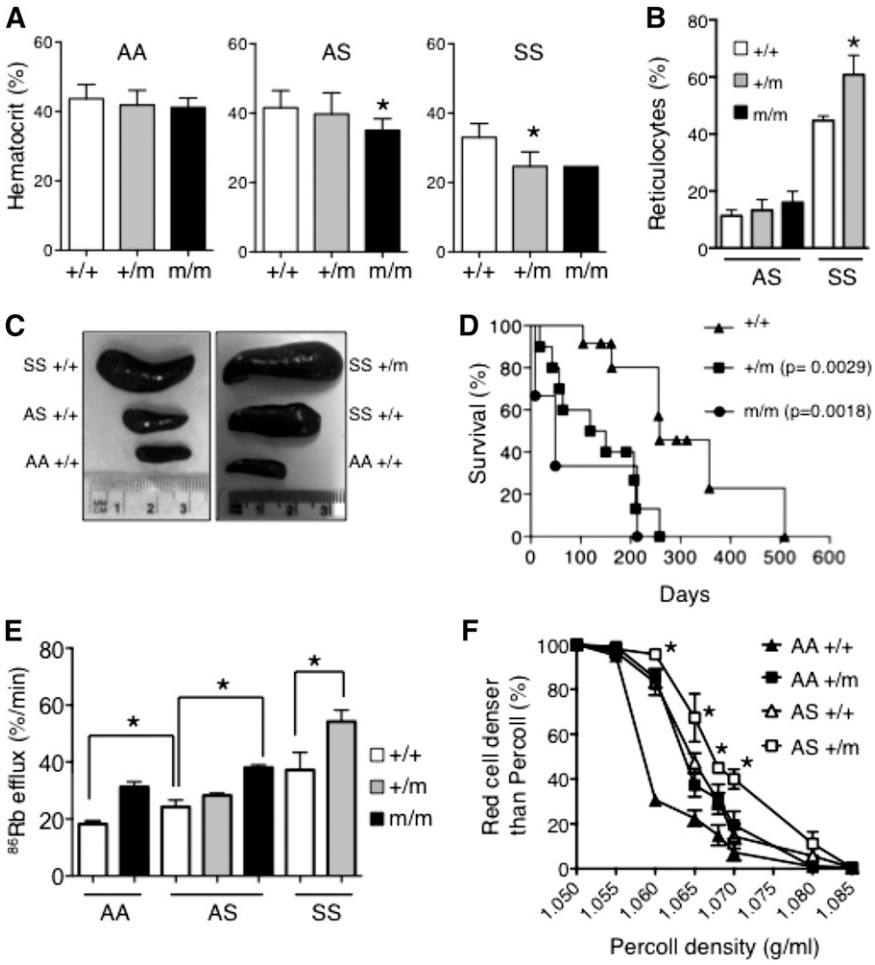

Figure 5. Effect of Kcc1 activation in sickle cell disease. (A) Hematocrits of 10-week-old mice. Mean ± SD of ≥5 mice for each genotype except $Hb^{SS}Kcc1^{M935K/M935K}$, which was a single animal. *$P < .05$ compared with $Kcc1^{+/+}$. (B) Percent reticulocytes in peripheral blood measured by thiazole orange. Mean ± SD of ≥3 mice for each genotype. *$P < .05$ compared with sickle homozygous (SS) $Kcc1^{+/+}$. (C) Representative spleens from 10-week-old mice with the stated genotypes. (D) Survival curves of homozygous sickle mice that are wild-type (+/+), heterozygous (+/m), or homozygous (m/m) for $Kcc1^{M935K}$. *P* values compared with $Kcc1^{+/+}$ mice were calculated using the log-rank (Mantel-Cox) test. (E) ^{86}Rb efflux from red cells of transgenic mice expressing wild-type adult human β-globin (AA), heterozygous for sickle cell mutation (AS), or homozygous for sickle cell mutation (SS) that are wild type (+/+), heterozygous (+/m), or homozygous (m/m) for $Kcc1^{M935K}$. *$P < .05$ compared with $Kcc1^{+/+}$. (F) Effect of heterozygous $Kcc1^{M935K}$ (+/m) on red cell densities of wild-type (AA), and heterozygous sickle (AS) mice determined by centrifugation through Percoll mixture of defined density. Student *t* test: $AS^{+/m}$ compared with $AS^{+/+}$, *$P < .05$.

activity worsens hemolysis, end-organ damage, and survival in a humanized mouse model of SCD.

KCC1 and KCC3 are the predominant K-Cl cotransporters in red cells.[2] Deletion of *Kcc1* and *Kcc3* genes in mice leads to macrocytic red cells with increased osmotic fragility and reduced ^{86}Rb efflux.[3] This phenotype is in direct contrast to that seen in $Kcc1^{M935K}$ mice, supporting the conclusion that activation of Kcc1 is the cause of the microcytic red cells. $Kcc1^{M935K}$ red cells are also hypochromic, which could not be explained by iron deficiency or defects in globin chain synthesis. However, mapping demonstrated that the microcytic phenotype was linked to chromosome 8 between 108.31 and 109.15 Mb, a region that does not contain any genes implicated

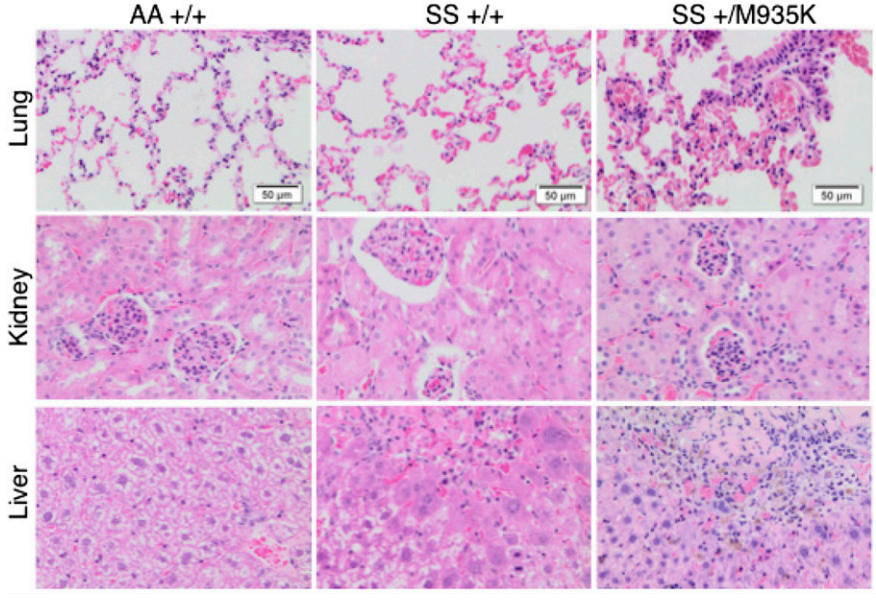

Figure 6. Activated Kcc1 cotransporter promotes end-organ damage in sickle cell disease. Histologic sections of lung, kidney, and liver stained with hematoxylin and eosin. Tissues were harvested from 10-week-old wild-type mice ($AA^{+/+}$), sickle homozygous mice ($SS^{+/+}$), and sickle homozygous with heterozygous Kcc1 mutation ($SS^{+/M935K}$). Sections are representative of 3 mice of each genotype.

in trans to globin expression, and high-performance liquid chromatography showed no alteration in α and β globin levels. Interestingly, red cells lacking Kcc1 have elevated MCH,[3] suggesting that altered Kcc1 activity in itself may regulate red cell hemoglobin content, although a direct linear relationship exists between MCV and MCH over a wide range of MCV values.

This study provides an example of the power of forward genetic screens in mice, especially now with current sequencing technology that enables rapid mutation detection. In this case, ENU mutagenesis has uncovered a highly conserved residue that controls phosphorylation of nearby threonines in Kcc1 and Kcc3. In the absence of a crystal structure of the KCCs, we can only speculate that the mutation perturbs structure (being a nonconservative hydrophobic to polar substitution), and accordingly, influences the accessibility of the nearby key phosphorylation sites that are important for channel regulation. This hypothesis has been previously proposed to explain changes in KCC activity seen with other point mutations in the cytoplasmic tail of KCC2.[18]

Red blood cell hydration is a major determinant of intracellular HbS concentration and polymer formation. Increased activity of KCC in sickle red cells is in part explained by the reticulocytosis, but may also be due to higher oxidant stress of HbSS red cells leading to sulfhydryl oxidation.[12,19] The molecular targets of sulfhydryl oxidation are unknown but could potentially include cysteines within KCC1 leading to conformational changes analogous to point mutations. Irrespective of the mechanism, it has been proposed that increased KCC activity might contribute to the pathogenesis of sickle cell disease and could therefore be a therapeutic target. However, this hypothesis has not been directly addressed using an in vivo model of SCD. Mating the $Kcc1^{M935K}$ mice with the fully humanized mouse model of SCD provided a unique opportunity to directly determine whether increased KCC activity worsens end-organ damage in SCD. Given the mixed genetic background, it is possible that the more severe sickle phenotype in mice carrying the mutant Kcc1 allele was due to another independent modifying BALB/c allele; however, this seems unlikely because the more severe sickle phenotype was always associated with the mutant Kcc1 allele, which was generated on a C57BL/6J background. Our findings of increased tissue damage and shortened survival with a modest increase in KCC1 activity (~30%) strengthens the impetus for identifying inhibitors of specific phosphatases that dephosphorylate these key regulatory threonines.

Acknowledgments

The authors thank Professor Doug Hilton and Dr Gerhard Rank for helpful discussions with mapping the mutation and The Australian Phenomics Network for sequence alignments.

This study was supported by a project grant (382900) from the Australian National Health and Medical Research Council (to S.M.J. and D.J.C.) and a Viertel Senior Medical Research fellowship (to D.J.C.).

Authorship

Contribution: F.C.B., B.T.K., S.M.J., J.S.W., and D.J.C. designed the research; F.C.B., A.J.C., J.E.C., C.M., and L.C., performed experiments; and F.C.B., S.M.J., and D.J.C. wrote the manuscript.

Conflict-of-interest disclosure: The authors declare no competing financial interests.

Correspondence: David J. Curtis, Australian Centre for Blood Diseases, Central Clinical School, Monash University, Alfred Centre, 99 Commercial Rd, Melbourne, VIC 3004, Australia; e-mail: david.curtis@monash.edu.

References

1. Gamba G. Molecular physiology and pathophysiology of electroneutral cation-chloride cotransporters. *Physiol Rev.* 2005;85(2):423-493.
2. Pan D, Kalfa TA, Wang D, et al. K-Cl cotransporter gene expression during human and murine erythroid differentiation. *J Biol Chem.* 2011;286(35):30492-30503.
3. Rust MB, Alper SL, Rudhard Y, et al. Disruption of erythroid K-Cl cotransporters alters erythrocyte volume and partially rescues erythrocyte dehydration in SAD mice. *J Clin Invest.* 2007; 117(6):1708-1717.
4. Bize I, Güvenç B, Robb A, Buchbinder G, Brugnara C. Serine/threonine protein phosphatases and regulation of K-Cl cotransport in human erythrocytes. *Am J Physiol.* 1999; 277(5 Pt 1):C926-C936.
5. de Los Heros P, Kahle KT, Rinehart J, et al. WNK3 bypasses the tonicity requirement for K-Cl cotransporter activation via a phosphatase-dependent pathway. *Proc Natl Acad Sci USA.* 2006;103(6):1976-1981.
6. Mercado A, Broumand V, Zandi-Nejad K, Enck AH, Mount DB. A C-terminal domain in KCC2 confers constitutive K+-Cl- cotransport. *J Biol Chem.* 2006;281(2):1016-1026.
7. Shen MR, Chou CY, Hsu KF, et al. The KCl cotransporter isoform KCC3 can play an important role in cell growth regulation. *Proc Natl Acad Sci USA.* 2001;98(25):14714-14719.
8. Rinehart J, Maksimova YD, Tanis JE, et al. Sites of regulated phosphorylation that control K-Cl cotransporter activity. *Cell.* 2009;138(3):525-536.
9. Kahle KT, Rinehart J, de Los Heros P, et al. WNK3 modulates transport of Cl- in and out of cells: implications for control of cell volume and neuronal excitability. *Proc Natl Acad Sci USA.* 2005;102(46):16783-16788.
10. de Los Heros P, Alessi DR, Gourlay R, et al. The WNK-regulated SPAK/OSR1 kinases directly phosphorylate and inhibit the K+-Cl- co-transporters. *Biochem J.* 2014;458(3):559-573.
11. Canessa M, Spalvins A, Nagel RL. Volume-dependent and NEM-stimulated K+,Cl- transport is elevated in oxygenated SS, SC and CC human red cells. *FEBS Lett.* 1986;200(1):197-202.
12. Joiner CH, Rettig RK, Jiang M, Franco RS. KCl cotransport mediates abnormal sulfhydryl-dependent volume regulation in sickle reticulocytes. *Blood.* 2004;104(9):2954-2960.
13. Trudel M, De Paepe ME, Chrétien N, et al. Sickle cell disease of transgenic SAD mice. *Blood.* 1994; 84(9):3189-3197.
14. Boettger T, Rust MB, Maier H, et al. Loss of K-Cl co-transporter KCC3 causes deafness, neurodegeneration and reduced seizure threshold. *EMBO J.* 2003;22(20):5422-5434.
15. Brown FC, Scott N, Rank G, et al. ENU mutagenesis identifies the first mouse mutants reproducing human β-thalassemia at the genomic level. *Blood Cells Mol Dis.* 2013;50(2): 86-92.
16. Rank G, Sutton R, Marshall V, et al. Novel roles for erythroid Ankyrin-1 revealed through an ENU-induced null mouse mutant. *Blood.* 2009; 113(14):3352-3362.
17. Wu LC, Sun CW, Ryan TM, Pawlik KM, Ren J, Townes TM. Correction of sickle cell disease by homologous recombination in embryonic stem cells. *Blood.* 2006;108(4):1183-1188.
18. Bergeron MJ, Gagnon E, Caron L, Isenring P. Identification of key functional domains in the C terminus of the K+-Cl- cotransporters. *J Biol Chem.* 2006;281(23):15959-15969.
19. Joiner CH, Rettig RK, Jiang M, Risinger M, Franco RS. Urea stimulation of KCl cotransport induces abnormal volume reduction in sickle reticulocytes. *Blood.* 2007; 109(4):1728-1735.